24GHz active retrodirective antenna array

Tzung-Jir Hong and Shyh-Jong Chung

A 24GHz active Van Atta planar antenna array proposed for increasing the vehicle radar echo in a vehicle collision avoidance system is designed and demonstrated. The antenna array contains two parallel linear sub-arrays. Each sub-array is composed of four receiving microstrip antennas, four transmitting microstrip antennas and four transistor amplifiers. At the angles of $-40° < \theta < 40°$, except those very close to the specular direction ($\theta = 0°$), the measured backscattering field levels of the fabricated array have variations < 3dB and are at least 10dB higher than those of a metal plate of the same size.

Introduction: The Van Atta retrodirective antenna array [1] possesses the advantage that the reradiated fields from all the transmitting elements of the array have a coherent phase in the arrival direction of an incident wave, thus yielding a broad backscattering field pattern. With this advantage, it has been suggested [2] that planar Van Atta arrays be equipped on vehicle bodies to increase the radar echoes in a vehicle collision avoidance system [3, 4]. In this Letter, a 24GHz active Van Atta microstrip antenna array is developed and demonstrated. As shown in Fig. 1, the array contains two parallel linear sub-arrays, with each sub-array formed by four active microstrip antenna pairs. Each antenna pair, e.g. pair 1-1′, is composed of a receiving antenna (antenna 1), a transmitting antenna (antenna 1′), and a transistor amplifier incorporated in the midway of a microstrip line connecting the two antennas. The transmitting antennas have the same polarisation as the receiving antennas. The signal captured by each receiving antenna is enlarged by the amplifier and is then re-transmitted by the corresponding transmitting antenna.

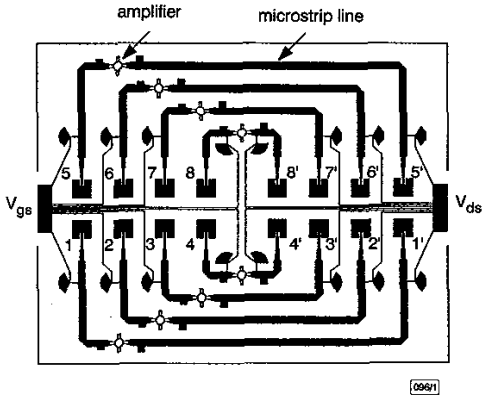

Fig. 1 *24 GHz active Van Atta microstrip antenna array*

Pathces 1 to 8 are receiving antennas and patches 1′ to 8′ are transmitting antennas

Design: To create a coherent phase at the wave arrival direction, the four transmitting antennas in each sub-array should have inter-element distances the same as those of the receiving antennas. Also, the phase delays in all the antenna pairs, from one receiving antenna, through the amplifier, to the corresponding transmitting antenna, should be the same or have differences equal to multiples of 360°. Here, the inter-element distances between the receiving (transmitting) antennas in each sub-array were chosen as 8.65mm (0.7 λ), which were the same as that between the two sub-arrays. To reduce the feedback coupling and avoid oscillation, the distance between the nearest-spaced paired antennas (i.e. antennas 4, 4′ and antennas 8, 8′) was selected as 14.83mm (1.2λ). The size of the whole array was measured to be $85 \times 67.5\text{mm}^2$.

The microstrip antennas were fabricated on a substrate of ε_r = 2.2 (dielectric constant) and t = 20mil (thickness) and had a geometry as shown in the inset of Fig. 2*a*. A narrow microstrip line (0.5mm wide) with impedance $Z_2 = 92\Omega$ was inserted into a square patch of size $3.96 \times 3.96\text{mm}^2$ at a position with input impedance equal to 92Ω. A quarter-wave microstrip line with impedance $Z_1 = 68\Omega$ was then used to transform the impedance to $Z_0 = 50\Omega$. This design may reduce the step discontinuity radiation and the interaction between the patch and the wide 50 Ω input line (1.54mm wide). The measured return loss and H-plane radiation pattern of the fabricated microstrip antenna are shown in Fig. 2*a* and *b*, respectively. The return loss was < –20dB at the centre frequency of 24.3GHz, with a 10dB bandwidth of 2.7%. The 3dB radiation beamwidth at 24.3GHz was ~95°.

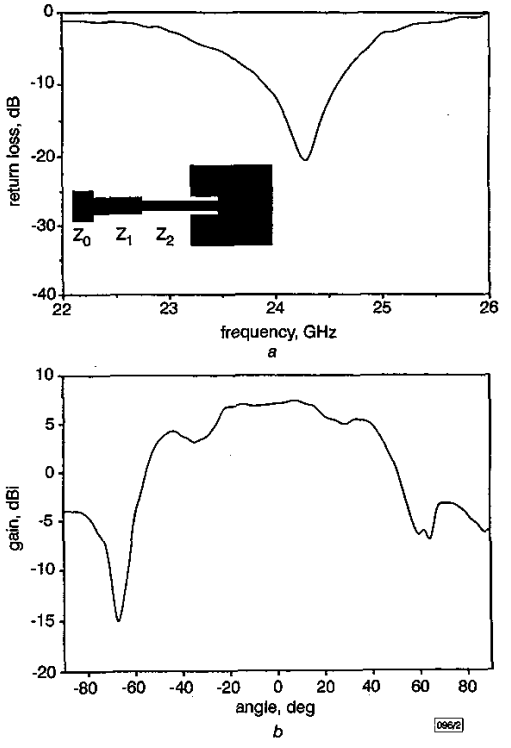

Fig. 2 *Measured return loss and H-plane radiation pattern of inset-fed microstrip antenna*

a Measured return loss
b H-plane radiation pattern
Z_o = 50 Ω, Z_1 = 68 Ω, Z_2 = 92 Ω

The amplifier was designed using the packaged NE42484C high electron mobility transistor (HEMT). Since no design data was available above 18GHz, the through-reflect-line (TRL) de-embedding method was first used to measure the scattering parameters of the HEMT from 18 to 30GHz. Discontinuity effects between the transistor terminals and microstrip lines were incorporated in the measurement so that the measured parameters could be directly used in the subsequent circuit design. The amplifier was designed using the commercial tool HP Series IV. Fig. 3 illustrates the measured results of the fabricated amplifier. The transistor was biased at V_{GS} = –0.2V and V_{DS} = 2V (I_D = 10mA). At a frequency of 24.3GHz, the amplifier gain was ~10dB and the return loss was –23dB.

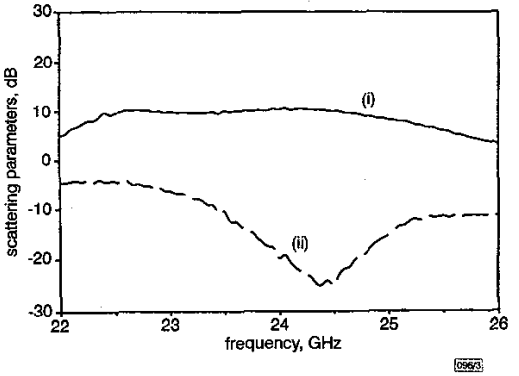

Fig. 3 *Measured gain (S_{21}) and return loss (S_{11}) of HEMT amplifier*

(i) S_{21}
(ii) S_{11}

Measurement results: The backscattering field pattern of the fabricated active retrodirective array was measured at a distance of 230cm using two closely spaced horn antennas. (The distance was larger than the far field distances for the antenna array and the measuring horn antennas.) Fig. 4 shows the results at 24.3GHz. As a comparison, the measured backscattering pattern of a metal plate of the same size as the array is also shown. The results were normalised to the backscattering field level of the metal plate at 0°. The array scattering pattern showed a narrow peak at 0°, which was due to the strong specular reflection of the array substrate ground. With the exception of this peak, the backscattering pattern of the array in the range –40° – 40° had variation < 3dB and was at least 10dB higher than that of the metal plate.

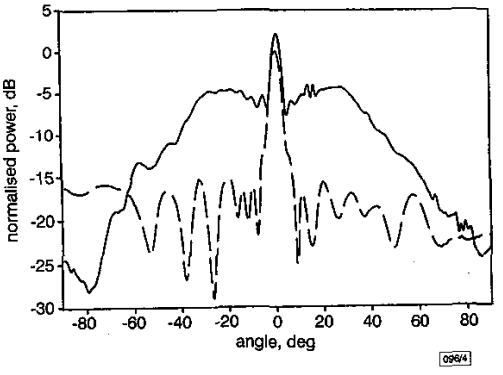

Fig. 4 *Measured backscattering field patterns of retrodirective array and metal plate*

——— retrodirective array
– – – metal plate

Conclusions: A 24GHz active Van Atta antenna array containing eight microstrip antenna pairs has been designed and demonstrated. A transistor amplifier with gain of 10dB was incorporated in each antenna pair to enhance the backscattering field level of the array. With the exception of a high peak in the specular direction, the backscattering field pattern of the array possessed a 3dB beamwidth of 80°. Within this beamwidth, the scattering field was at least 10dB higher than that of a metal plate of the same size.

Acknowledgment: This work was supported by the National Science Council of the Republic of China under grant NSC 89-2213-E-009-050.

26 August 1999
Electronics Letters Online No: 19991223
DOI: 10.1049/el:19991223

Tzung-Jir Hong and Shyh-Jong Chung (*Department of Communication Engineering, National Chiao Tung University, 1001 Ta Hsueh Road, Hsinchu, Taiwan, Republic of China*)

E-mail: sjchung@cm.nctu.edu.tw

References

1 VAN ATTA, L.C.: 'Electromagnetic reflector'. U.S. Patent 2,908,002, Serial no. 514,040, October 1959

2 CHUNG, S.-J., and CHANG, K.: 'A retrodirective microstrip antenna array', *IEEE Trans. Antennas Propag.*, 1998, **46**, (12), pp. 1802–1809

3 MEINEL, H.H.: 'Commercial applications of millimeterwaves: History, present status, and future trends', *IEEE Trans. Microw. Theory Tech.*, 1995, **43**, (7), pp. 1639–1653

4 ZELUBOWSKI, S.A.: 'Low cost antenna alternatives for automotive radars', *Microw. J.*, 1994, **37**, (7), pp. 54–63

Conduction current crossing domain boundaries in heterogeneous hybrid computational electromagnetics formulation

M.A. Mangoud, R.A. Abd-Alhameed, P.S. Excell and J.A. Vaul

A heterogeneous hybrid computational electromagnetics method is presented that permits conduction currents to cross the boundary between different computational domains. The method uses a standard frequency-domain moment-method program and the finite-difference time-domain method to compute the fields in the two regions. Several validation cases are examined and the results compared with available data.

Introduction: Certain problems, notably those involving coupling of a mobile telephone to human tissue, require use of the finite-difference time-domain (FDTD) method for one part of the problem and the method of moments (MoM) for another. If conduction current is required to cross the boundary between the two methods, a special treatment is required to ensure current continuity across the surface. Earlier work [1 – 3] is extended for the case where the source region is subdivided, one part replaced by equivalent surface currents using the equivalence principle (computed by MoM) and the other part handled with the use of direct impressed currents (suitable to couple with FDTD). An industry-standard frequency-domain MoM programme [4] was used, to aid acceptance in practical applications.

Coupling between the scatterer and source regions is calculated using the reaction theorem, with appropriate modifications to the MoM program to take account of the fact that the basis and weighting functions are not the same.

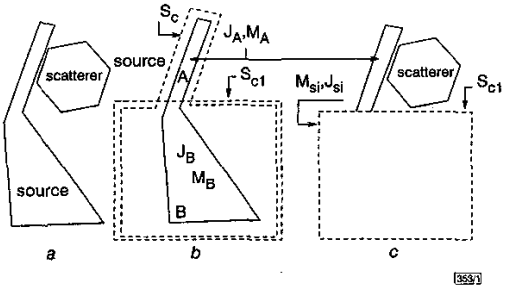

Fig. 1 *Basic geometry of problem*

a Source and scatterer regions
b Sub-regions A and B of source
c Equivalent surface for currents in sub-region B

Summary of method: Fig. 1*a* shows two regions, one enclosing the source, the other enclosing the scatterer. The source region is further subdivided into two sub-regions, A and B, as shown in Fig. 1*b*. The scatterer can be very close or attached to source region B if it has a dielectric surface. In general, there is no physical attachment between source region A and the scatterer region. The source region was modelled using MoM whereas the scatterer was modelled using FDTD. In Fig. 1*b*, the surface S_c encloses the entire source region. The fields due to the induced currents from both source sub-regions A and B over the closed surface S_{c1} can be computed in order to evaluate the surface currents J_{si} and M_{si}:

$$M_{si} = \hat{n} \times (E(J_A, M_A) + E(J_B, M_B))$$
$$J_{si} = (H(J_A, M_A) + H(J_B, M_B)) \times \hat{n} \qquad (1)$$

where J_A, J_B, M_A and M_B are the electric and magnetic currents of source regions A and B; and $\hat{n}$ is the unit vector normal to the surface S_{c1}. Now let the part of the surface S_c adjacent to sub-region A be coincident with the surface of the conducting source structure within A. The currents on S_c then become the surface currents on the conductor, which can be transferred to an FDTD model by treating them as impressed currents. The whole source region is then modelled using the FDTD method with impressed currents replacing sub-region A and a surface of equivalent currents replacing sub-region B (see Fig. 1*c*). The hard (impressed) sources for a perfectly conducting surface ($M_A = 0$) considered in region A can be given in FDTD as follows: